Supplemental Tables

Supplemental Table S1. Identity matrix between syntenic XyGUL GH5_4 enzymes and other specific previously characterized *endo*-xyloglucanases (1). Only amino acid sequences of the catalytic domains were used in the analysis. This data was generated with MatGAT (2), with percent similarity values in the lower left half and percent identity values in the upper right half of the table.

Protein name	*Bo*GH5	*Bc*GH5	*Bu*GH5	*Bf*GH5	*Dg*GH5	XEG5A	XEG5B	*Ppab*GH5	*Pbr*GH5
*Bo*GH5		36.4	31.7	36.1	45.1	29.9	32.1	33.7	29.8
*Bc*GH5	53.9		34.5	34.3	39.2	35.2	35.5	37.4	36.4
*Bu*GH5	50.7	48.4		59.5	46.5	31.5	39.4	35.2	32.8
*Bf*GH5	56.3	49.3	68.4		49.7	29.6	43	30.8	31.1
*Dg*GH5	62.5	53.6	60.1	65.8		32.1	39.2	33.8	29.9
XEG5A	50	50.7	46.9	48.2	52.9		31.7	30.2	32.4
XEG5B	51	50.3	52.9	60.9	59.6	51		31.5	30.8
*Ppab*GH5	51.3	54.2	54.5	47.8	53.6	51.4	51		31.5
*Pbr*GH5	47.4	49.7	48.1	47.8	49.2	51.2	45.5	49.2	

Supplemental Table S2. Identity matrix between syntenic XyGUL TBDTs (SusC homologs). This data was generated with MatGAT (2), with percent similarity values in the lower left half and percent identity values in the upper right half of the table.

Protein name	*Bo*TBDT	*Bc*TBDT	*Bu*TBDT	*Bf*TBDT	*Dg*TBDT
*Bo*TBDT		34.3	33.9	35.9	33.2
*Bc*TBDT	54.7		64.9	66.1	49.9
*Bu*TBDT	56.2	77.5		77.7	52.7
*Bf*TBDT	56.1	78.9	88.8		53.4
*Dg*TBDT	53.5	67.4	70.9	70.2	

Supplemental Table S3. Identity matrix between syntenic XyGUL SGBPs-A (SusD homologs). This data was generated with MatGAT (2), with percent similarity values in the lower left half and percent identity values in the upper right half of the table.

Protein name	*Bo*SGBP-A	*Bc*SGBP-A	*Bu*SGBP-A	*Bf*SGBP-A	*Dg*SGBP-A
*Bo*SGBP-A		20.1	21.5	20.4	21.2
*Bc*SGBP-A	40.8		42	41.5	38.5
*Bu*SGBP-A	41.3	58		58.6	47.5
*Bf*SGBP-A	41	59.9	72.8		51.3
*Dg*SGBP-A	41.3	54.4	62.8	67.1	

Supplemental Table S4. Identity matrix between syntenic XyGUL SGBPs-B. This data was generated with MatGAT (2), with percent similarity values in the lower left half and percent identity values in the upper right half of the table.

Protein name	*Bo*SGBP-B	*Bc*SGBP-B	*Bu*SGBP-B	*Bf*SGBP-B	*Dg*SGBP-B
*Bo*SGBP-B		15.6	17	18.7	18.5
*Bc*SGBP-B	29.9		56.4	29.4	21.8
*Bu*SGBP-B	29.9	69.7		29.6	23.3
*Bf*SGBP-B	31.3	46.3	46.2		32
*Dg*SGBP-B	30.5	38.7	39.8	53.1	

Supplemental Table S5. Identity matrix between syntenic XyGUL GH95 enzymes and other specific previously characterized α-1,2-fucosidases. This data was generated with MatGAT (2), with percent similarity values in the lower left half and percent identity values in the upper right half of the table.

Protein name	BuGH95[a]	BfGH95[a]	DgGH95[a]	BliGH95[b]	BbGH95[c]	CjGH95[d]	CpGH95[e]	BoGH95[f]
BuGH95[a]		81.3	45.1	29.8	14.1	36.4	20.9	35.5
BfGH95[a]	87.3		45.2	29.1	15.2	36.1	21.2	35.8
DgGH95[a]	61.5	60.8		28.8	14.3	37.1	22	35.5
BliGH95[b]	47	45.7	48.2		13.3	29	16.3	27.2
BbGH95[c]	21.9	22.9	22.4	21.1		15.7	20.7	14.4
CjGH95[d]	56	57.1	55.1	46.5	23.6		21.4	47.8
CpGH95[e]	31.6	32.5	33.1	26.8	35.5	32.6		21.8
BoGH95[f]	55.7	54.2	55	45.6	22.5	63.1	32.5	

[a]This study.
[b]*Bifidobacterium longum* subsp. infantis ATCC 15697, GenBank ACJ53393.1 (3)
[c]*Bifidobacterium bifidum* JCM 1254, GenBank AAQ72464.1 (4, 5)
[d]*Cellvibrio japonicus* Ueda107, GenBank ACE83895.1 (6)
[e]*Clostridium perfringens* ATCC 13124, GenBank ABG82552.1 (7)
[f] α-L-galactosidase from *Bacteroides ovatus* ATCC 8483, GenBank EDO10805.1 (8)

Supplemental Figures

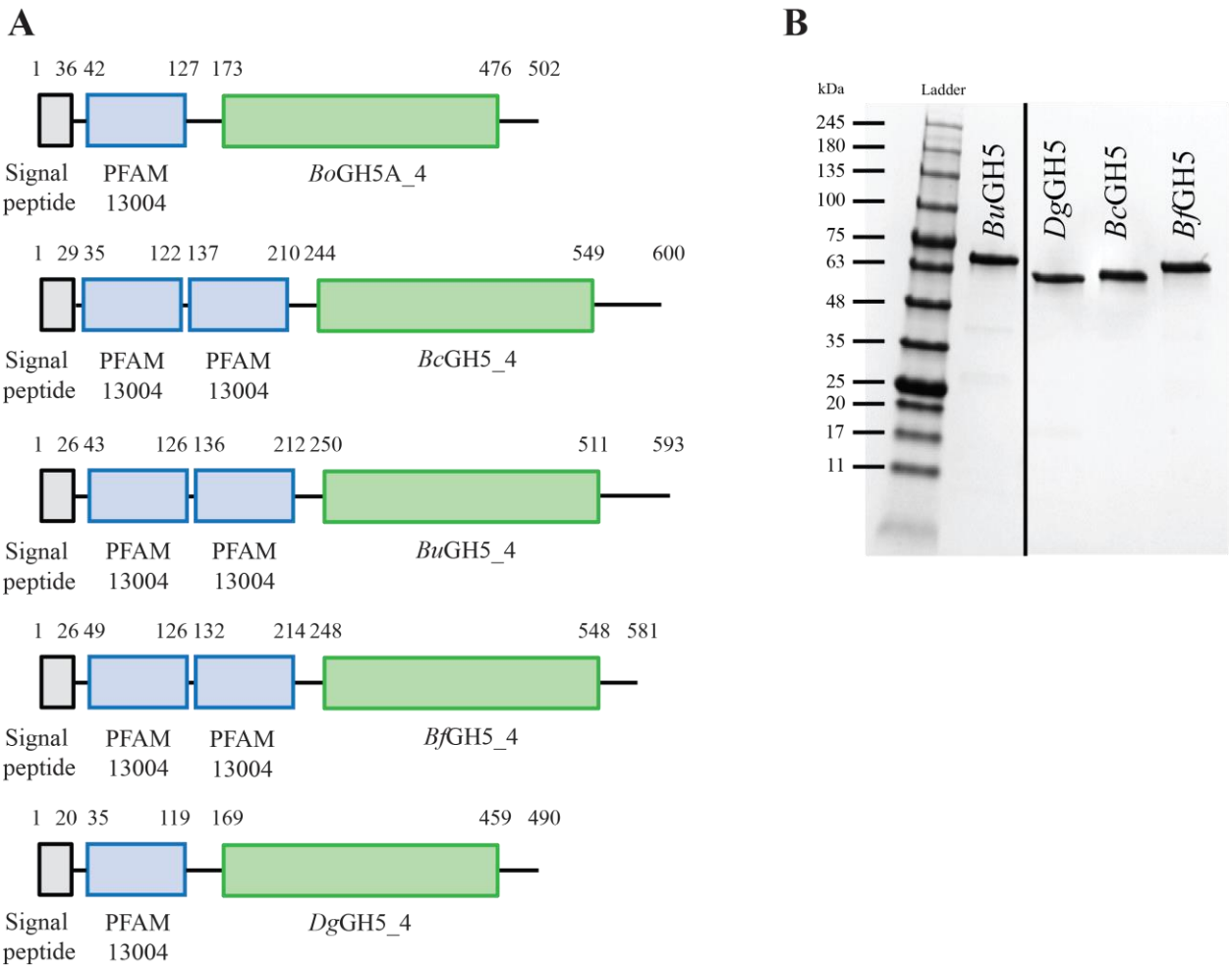

Figure S1. Modular architecture of the key *endo*-xyloglucanase GH5 gene products. (A) The full-length gene products are composed of a signal peptidase II signal peptide with lipidation site (Cys-1), one or two PFAM PF13004 domains, and a GH5 catalytic module. (B) SDS/PAGE of the purified full-length protein constructs.

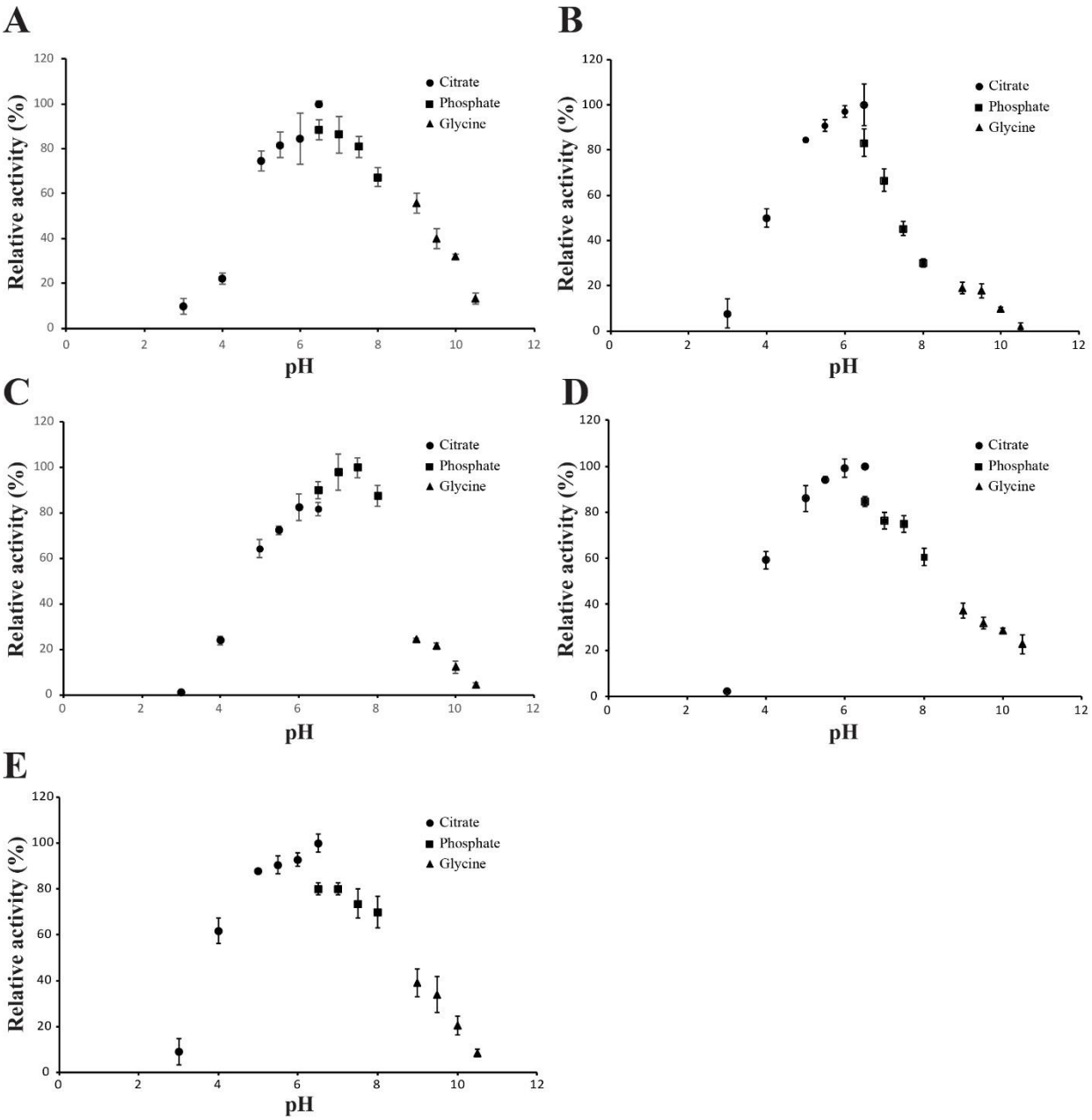

Figure S2. pH-rate profiles of recombinant XyGUL GH5 enzymes. A. *Bo*GH5A **B.** *Bu*GH5 **C.** *Bc*GH5 **D.** *Bf*GH5 **E.** *Dg*GH5 for tamXyG. Error bars represent standard errors of the mean for three replicates.

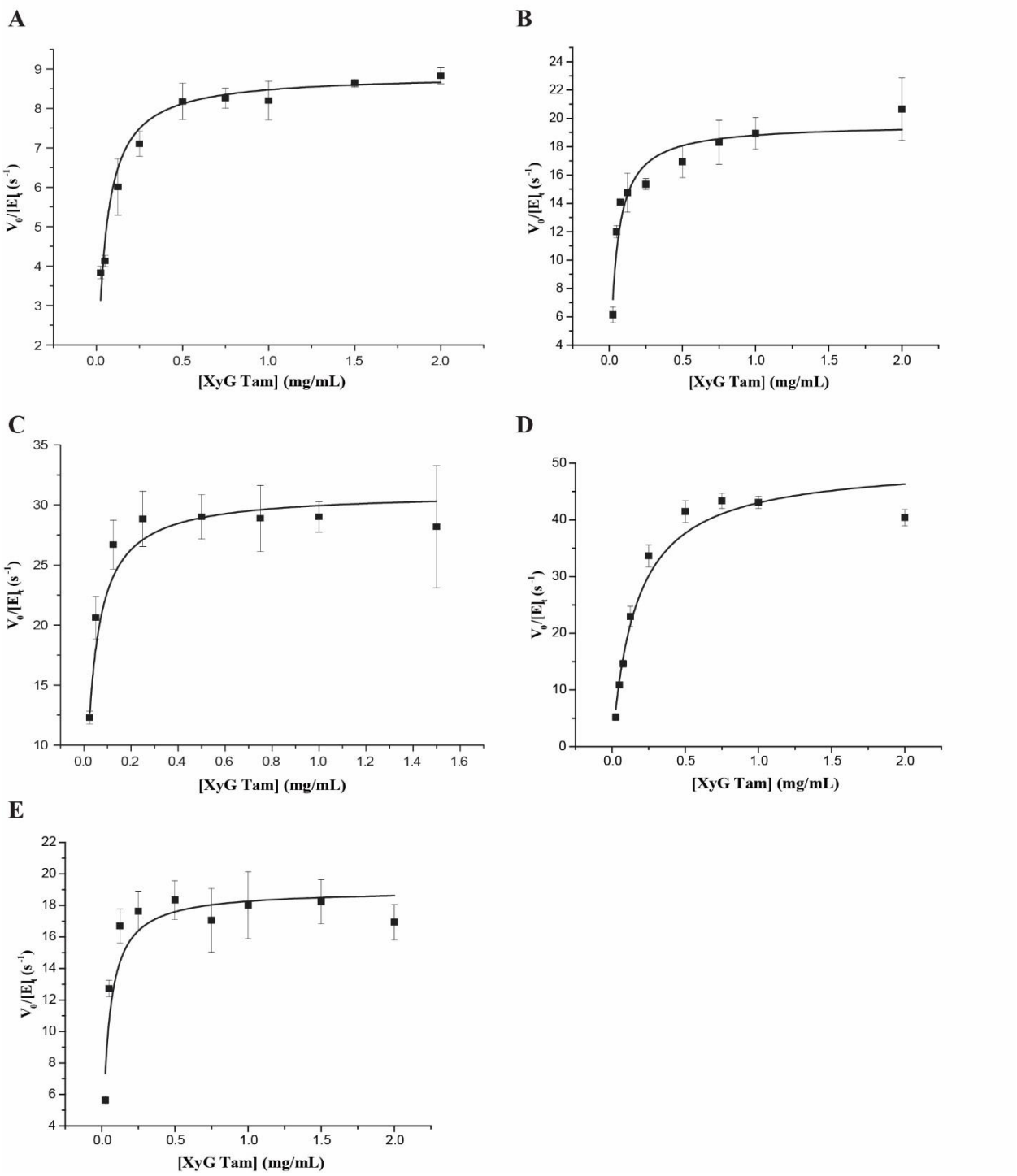

Figure S3. Initial-rate kinetics curves fitted to the Michaelis-Menten equation of **A.** *Bo*GH5A **B.** *Bu*GH5 **C.** *Bc*GH5 **D.** *Bf*GH5 **E.** *Dg*GH5 for tamXyG. Curve fitting was done on OriginPro 2015 and bars represent standard errors based on three replicates.

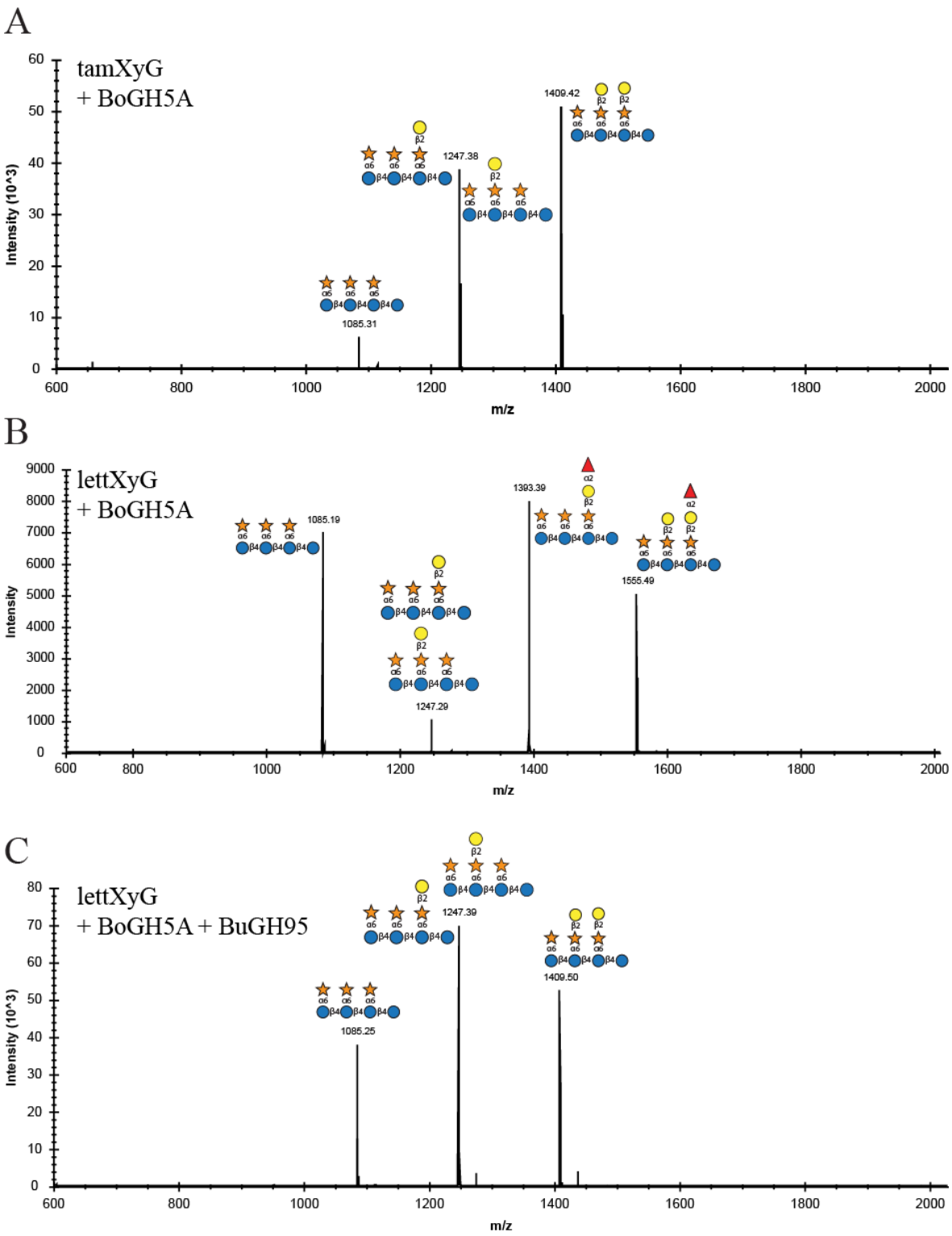

Figure S4. MALDI-TOF spectra of the products of *Bo*GH5A. A. tamXyG B. lettXyG and C. sequentially digested with *Bu*GH95 against lettXyG.

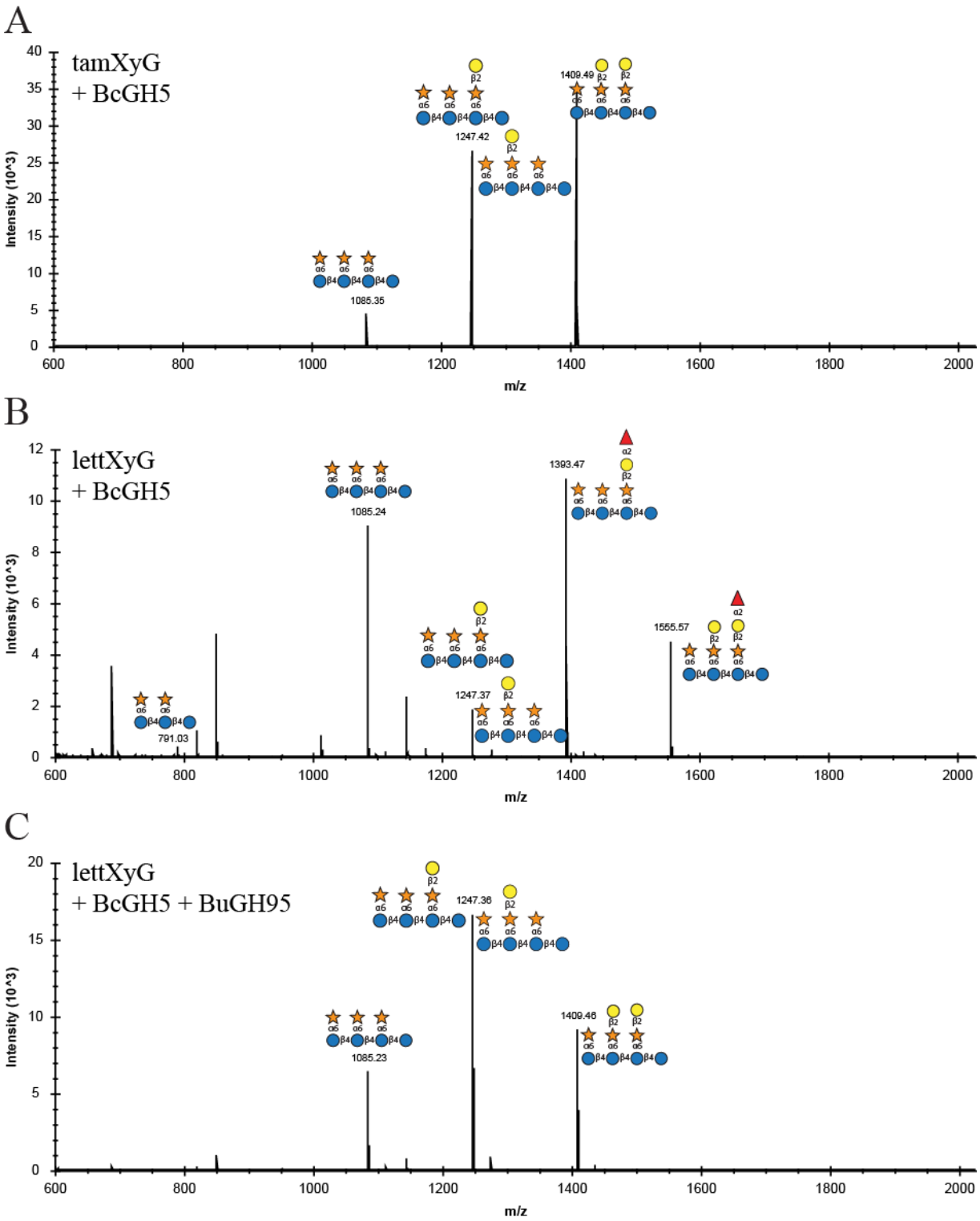

Figure S5. MALDI-TOF spectra of the products of *Bc*GH5. A. tamXyG B. lettXyG and C. sequentially digested with *Bu*GH95 against lettXyG.

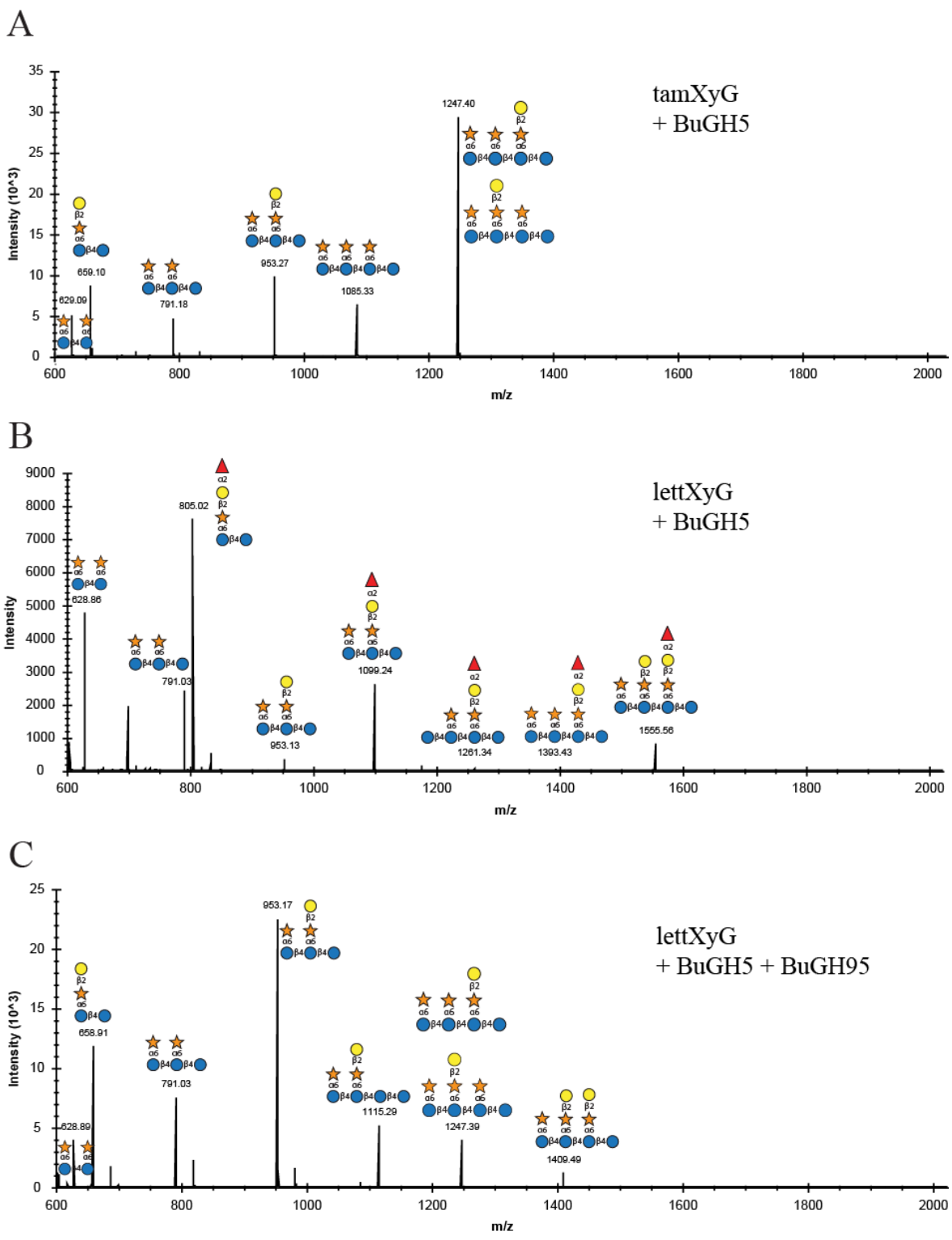

Figure S6. MALDI-TOF spectra of the products of *Bu*GH5. A. tamXyG B. lettXyG and C. sequentially digested with *Bu*GH95 against lettXyG.

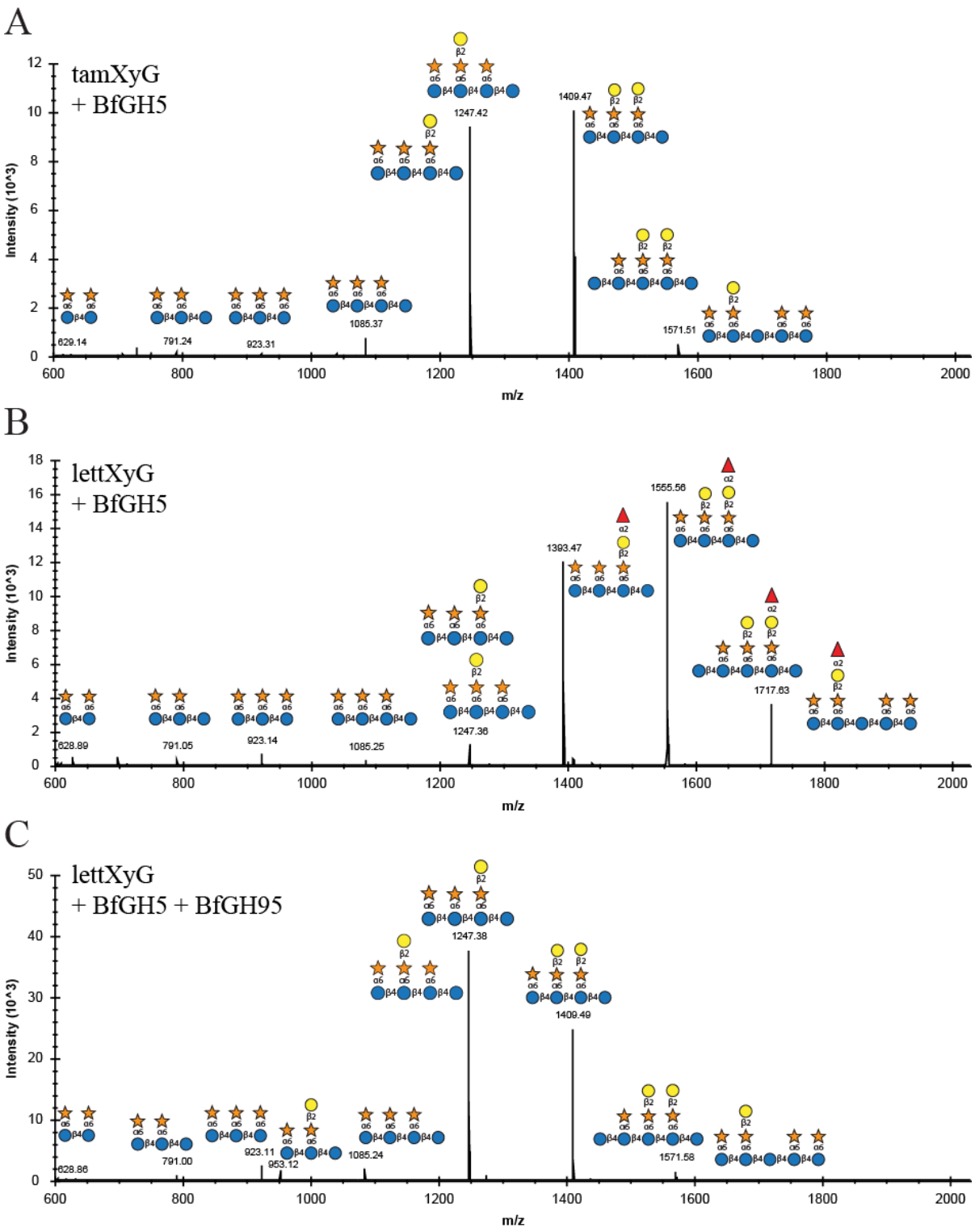

Figure S7. MALDI-TOF spectra of the products of *Bf*GH5. A. tamXyG B. lettXyG and C. sequentially digested with *Bf*GH95 against lettXyG.

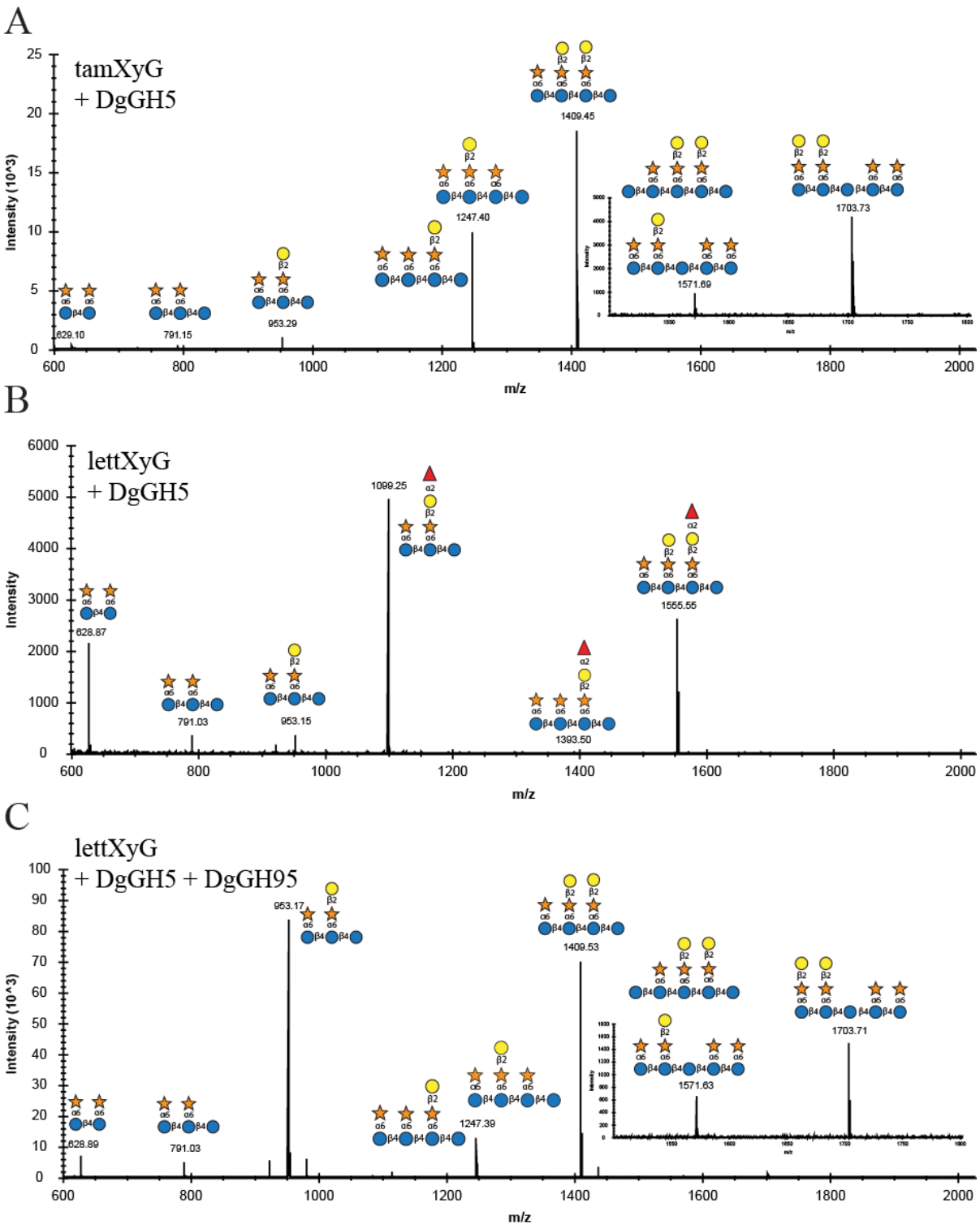

Figure S8. MALDI-TOF spectra of the products of *Dg*GH5. A. tamXyG B. lettXyG and C. sequentially digested with *Dg*GH95 against lettXyG.

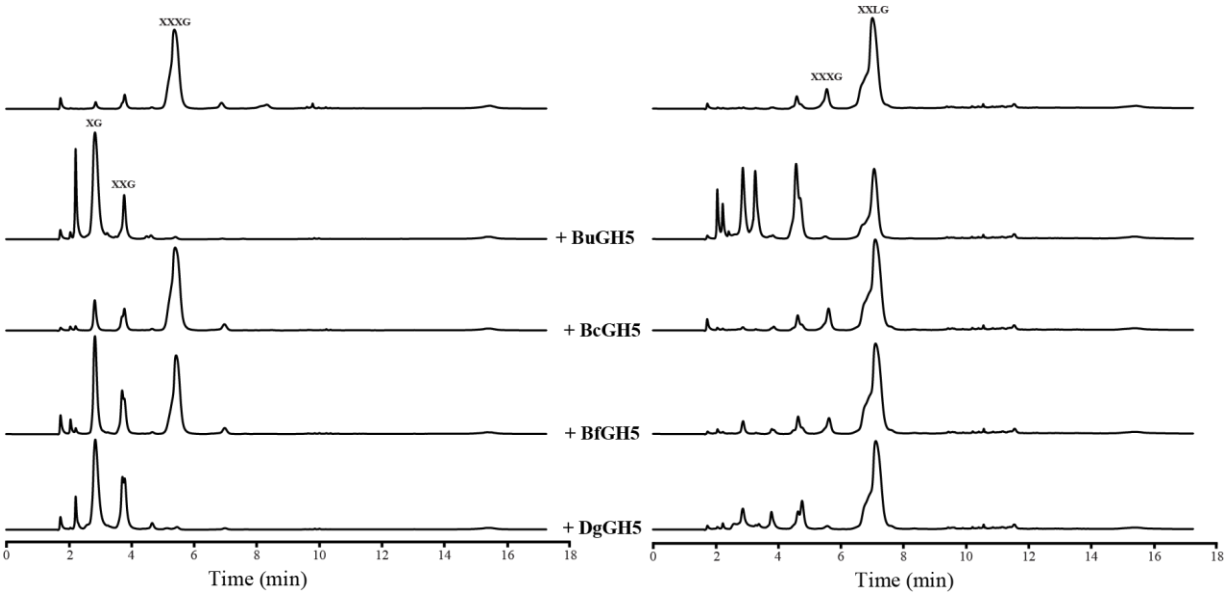

Figure S9. HPAEC-PAD analysis of the limit-digestion products of XXXG and XXLG by the key recombinant GH5 *endo*-xyloglucanases.

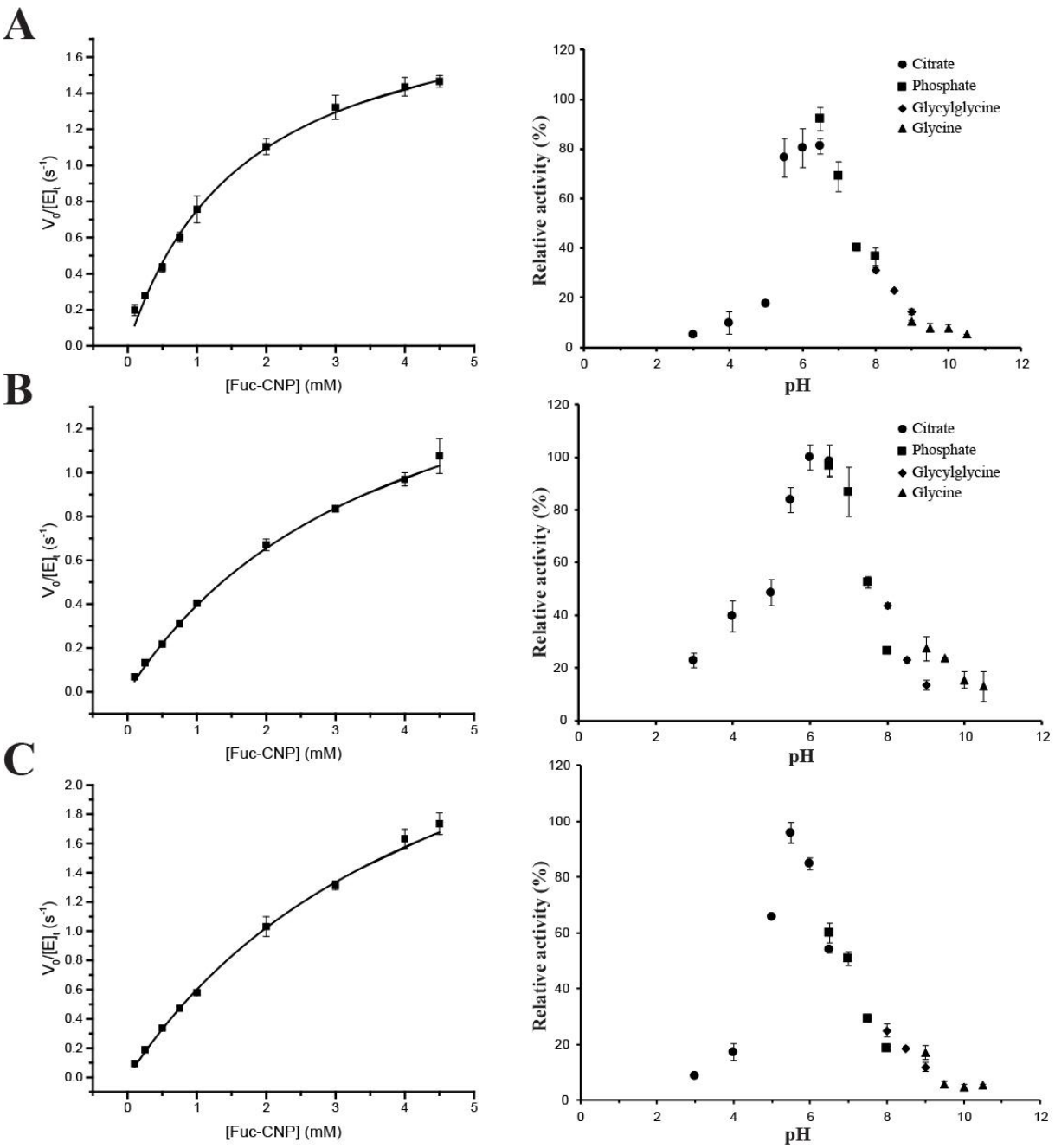

Figure S10. Initial-rate kinetics curves fitted to the Michaelis-Menten equation and pH optima of recombinant XyGUL GH95 recombinant enzymes. A. *Bu*GH95 **B.** *Bf*GH95 **C.** *Dg*GH95 for CNP-α-Fucose.

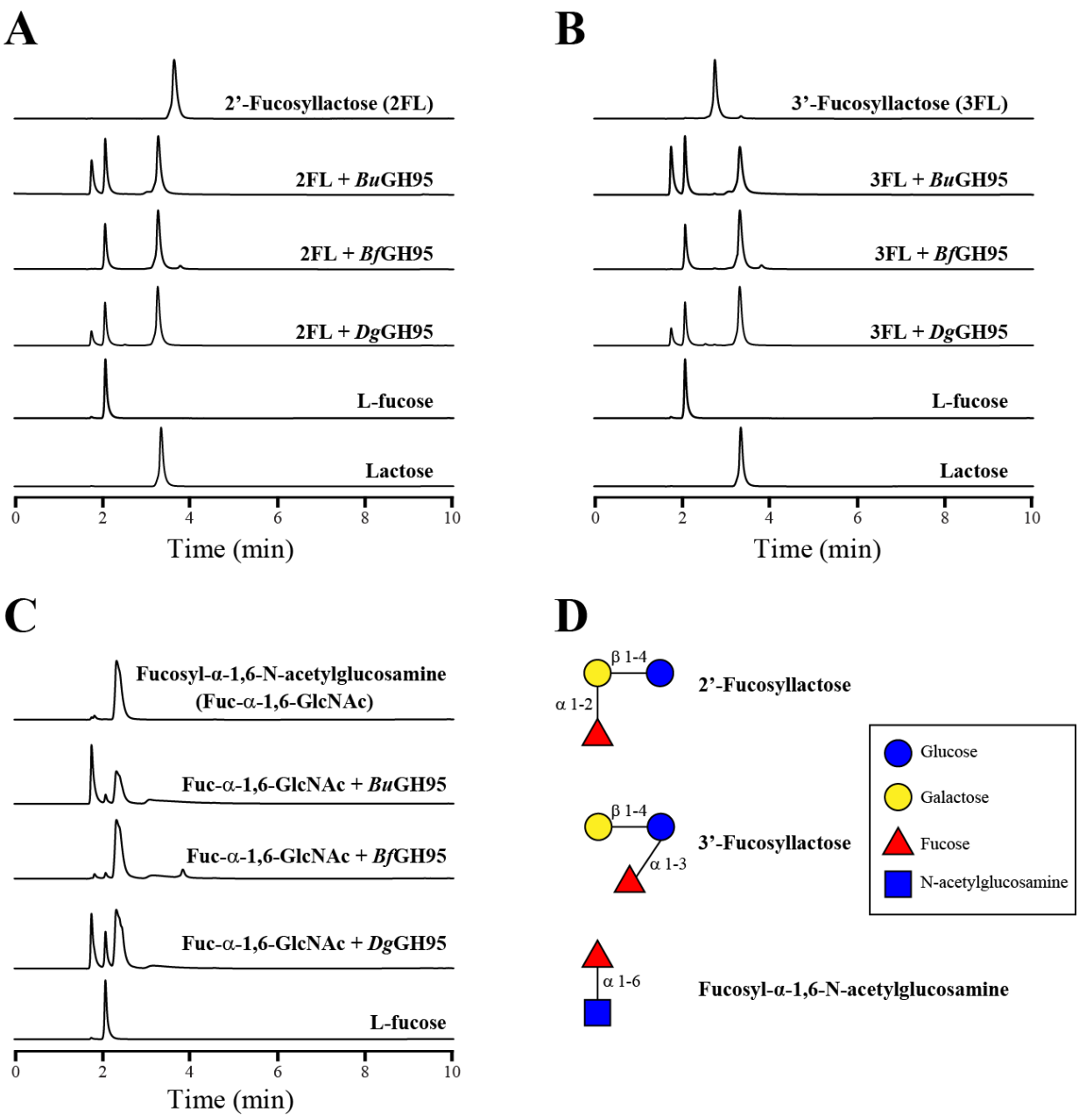

Figure S11. The product profile of fucosidases against fucose α-1,2/α-1,3/α-1,6 substrates. Recombinant *Bu*GH95, *Bf*GH95, and *Dg*GH95 were incubated with **A.** 2'-Fucosyllactose **B.** 3'-Fucosyllactose **C.** Fucosyl-α-1,6-N-acetylglucosamine. **D.** Chemical structure of the different fucosyl substrates.

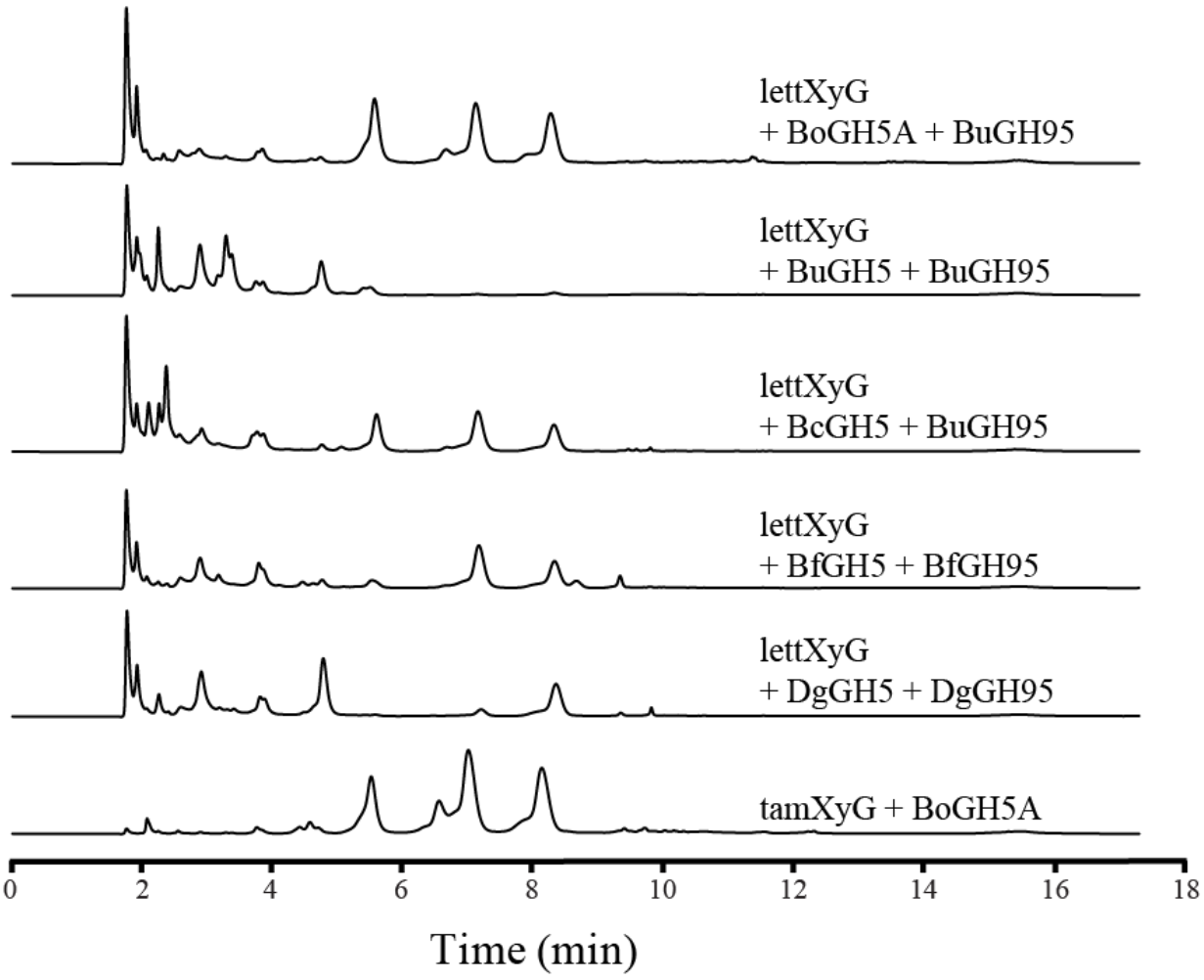

Figure S12. Product analysis by HPAEC-PAD of fucosylated lettXyG hydrolyzed by XyGUL-encoded GH5_4 *endo*-xyloglucanases and GH95 α-fucosidases.

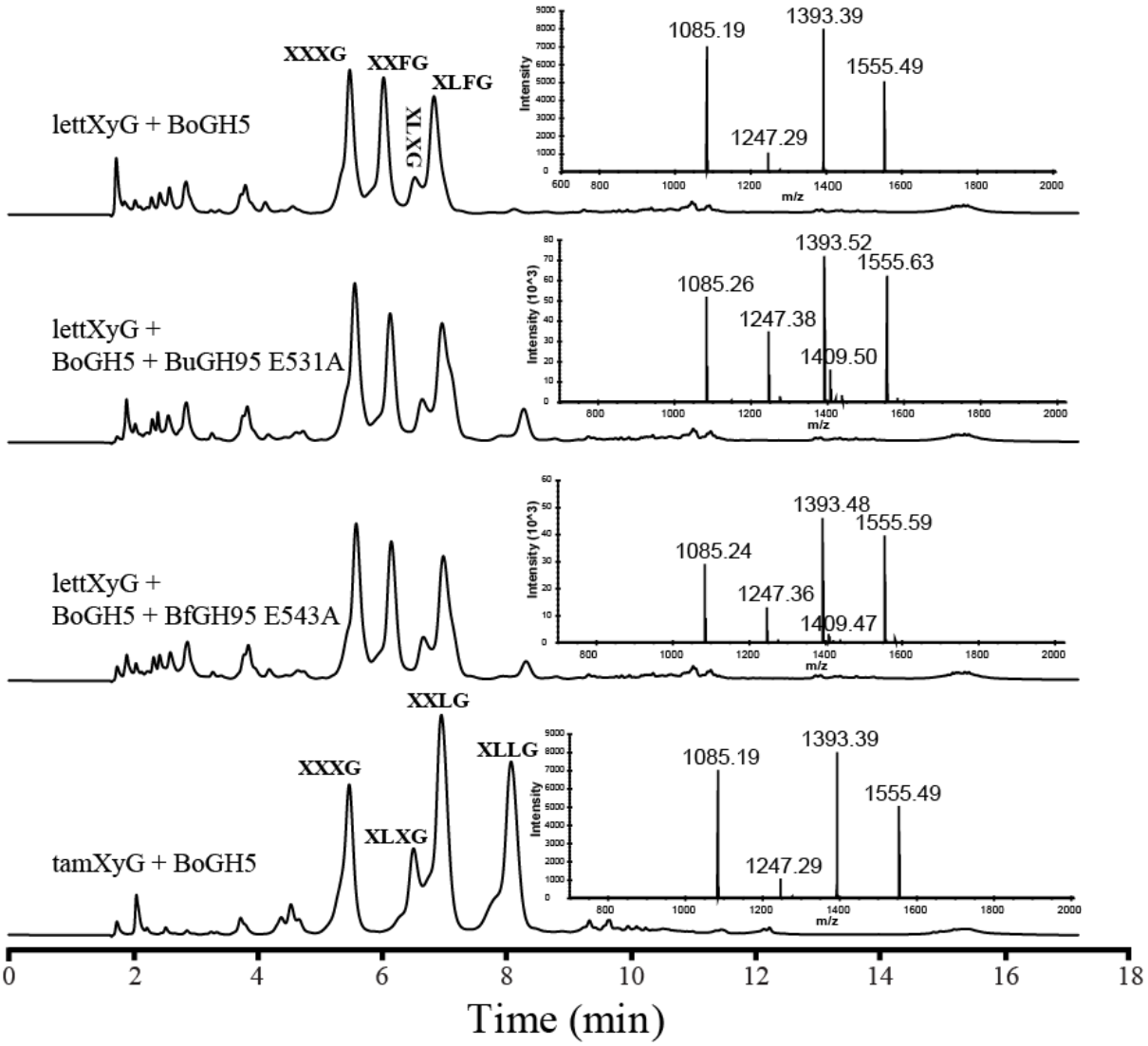

Figure S13. The product profile of general acid mutants *Bu*GH95 E531A and *Bf*GH95 E543A against fucosylated xyloglucan oligosaccharides. Fucosylated xyloglucan oligosaccharides mixture (XXXG, XXFG, XLXG, and XLFG) were produced by the action of *Bo*GH5A on lettXyG and subsequently incubated as a starting material with 2 μM of the recombinant *Bu*GH95 E531A and *Bf*GH95 E543A at 37 ºC for 22h in 50 mM sodium citrate buffer, pH 6.0.

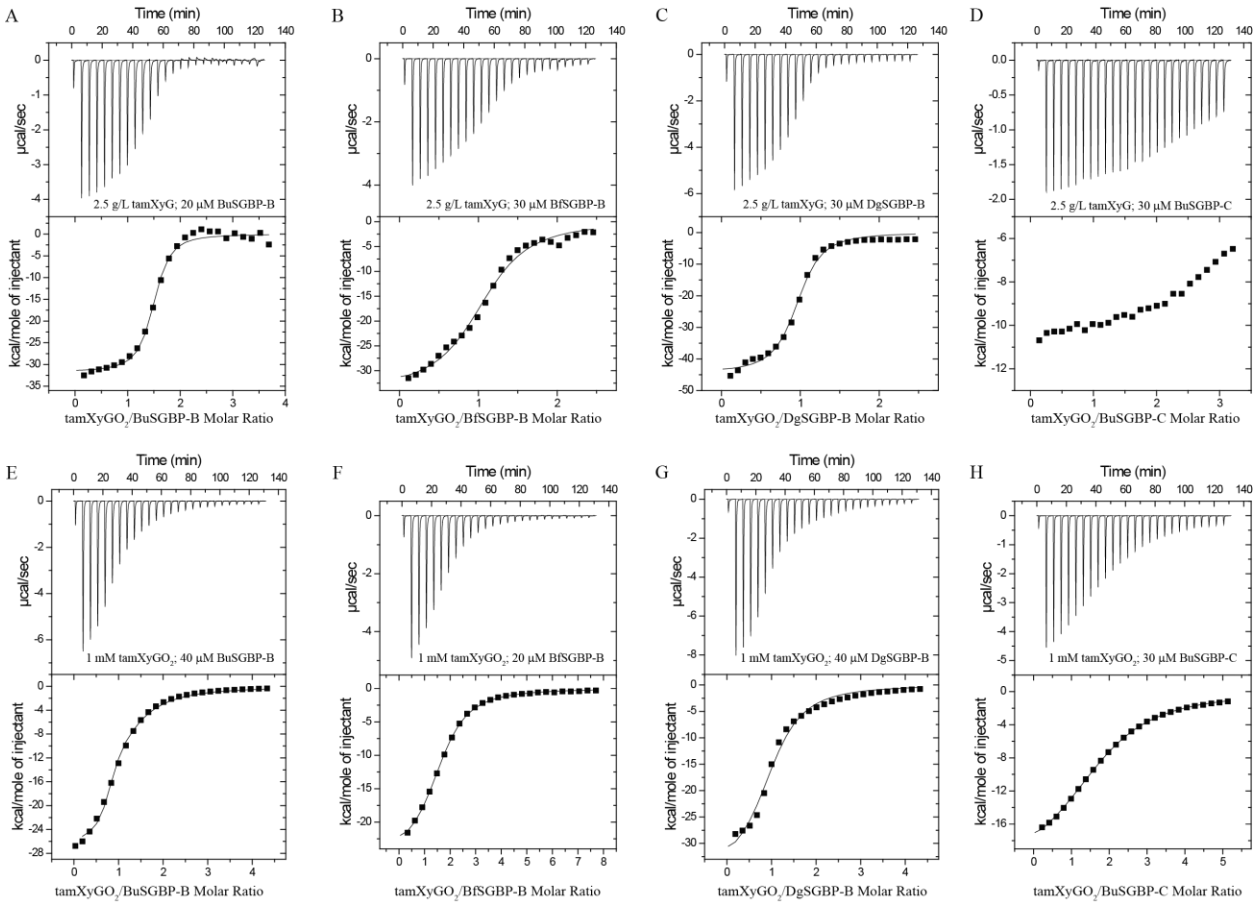

Figure S14. Representative isothermal titration calorimetry (ITC) results for SGBP-B and *Bu*SGBP-C titrations with tamXyG and tamXyGO$_2$. All titrations were performed in 50 mM Sodium Phosphate (pH 7.0) at 25°C. In each case, the upper graph shows the raw injection heat signal, and the bottom graph shows the integrated data and, where appropriate, fits to a 1:1 binding model. Concentrations of the protein and glycan are indicated on the upper panel. (A) *Bu*SGBP-B with tamXyG; (B) *Bf*SGBP-B with tamXyG; (C) *Dg*SGBP-B with tamXyG; (D) *Bu*SGBP-C with tamXyG; (E) *Bu*SGBP-B with tamXyGO$_2$; (F) *Bf*SGBP-B with tamXyGO$_2$; (G) *Dg*SGBP-B with tamXyGO$_2$; (H) *Bu*SGBP-C with tamXyGO$_2$.

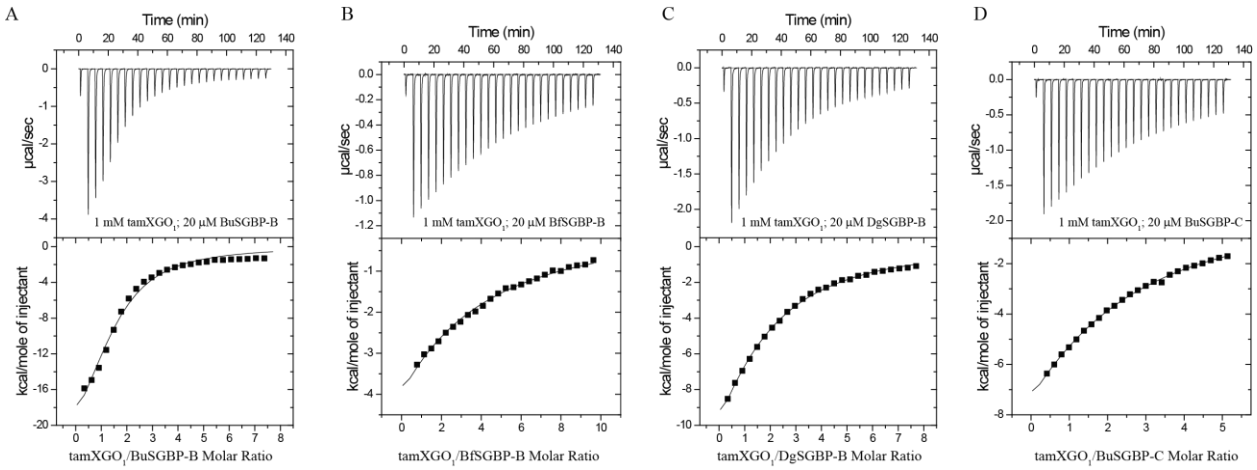

Figure S15. Representative isothermal titration calorimetry (ITC) results for SGBP-B and *Bu*SGBP-C titrations with tamXyGO$_1$ produced by the action of *Bo*GH5A on tamXyG. All titrations were performed in 50 mM Sodium Phosphate (pH 7.0) at 25°C. In each case, the upper graph shows the raw injection heat signal, and the bottom graph shows the integrated data and, where appropriate, fits to a 1:1 binding model. Concentrations of the protein and glycan are indicated on the upper panel. (A) *Bu*SGBP-B with tamXyGO$_1$; (B) *Bf*SGBP-B with tamXyGO$_1$; (C) *Dg*SGBP-B with tamXyGO$_1$; (D) *Bu*SGBP-C with tamXyGO$_1$.

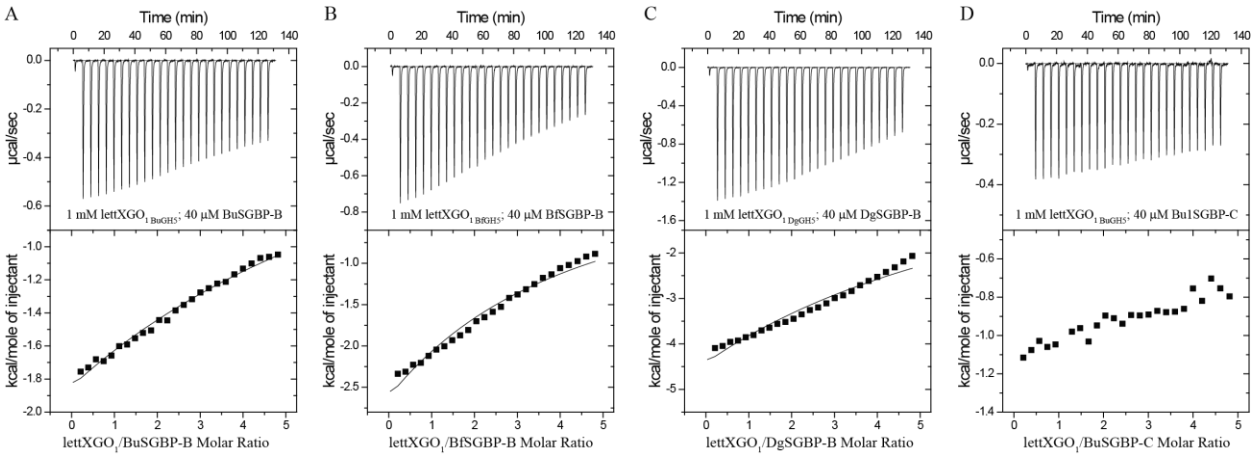

Figure S16. Representative isothermal titration calorimetry (ITC) results for SGBP-B and *Bu*SGBP-C titrations with lettXyGO$_1$ produced by the action of their cognate GH5 on lettXyG. All titrations were performed in 50 mM Sodium Phosphate (pH 7.0) at 25°C. In each case, the upper graph shows the raw injection heat signal, and the bottom graph shows the integrated data and, where appropriate, fits to a 1:1 binding model. Concentrations of the protein and glycan are indicated on the upper panel. (A) *Bu*SGBP-B with lettXyGO$_{1\ BuGH5}$; (B) *Bf*SGBP-B with lettXyGO$_{1\ BfGH5}$; (C) *Dg*SGBP-B with lettXyGO$_{1\ DgGH5}$; (D) *Bu*SGBP-C with lettXyGO$_{1\ BuGH5}$.

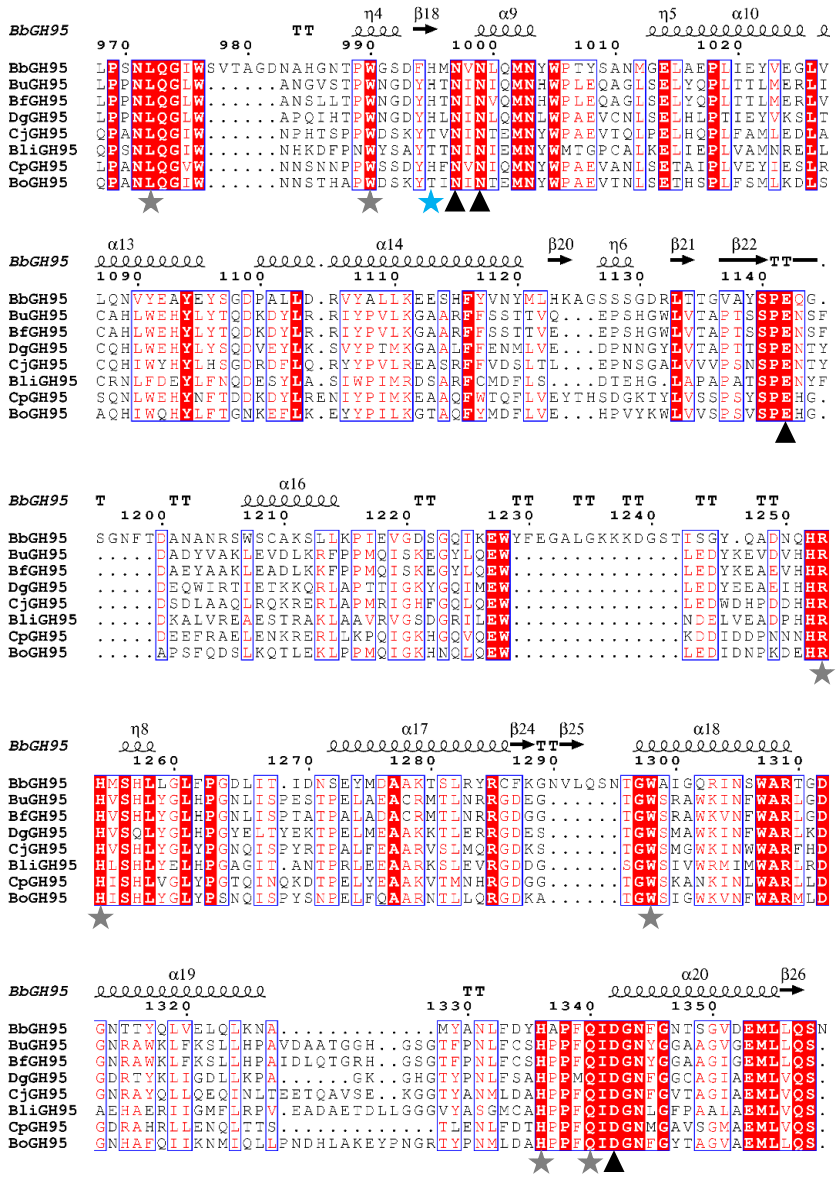

Figure S17. Structure-based protein sequence alignment of representative GH95 members. See Table S5 for enzyme abbreviations, accession numbers, and references. Conserved residues are highlighted in red. Black triangles indicate the amino acid residues that are involved in catalytic reaction. Grey stars indicate the amino acid residues that are involved in substrate recognition. Light blue star refers to the threonine residue of *Bo*GH95 α-L-galactosidase (encoded by BACOVA_03438) that makes direct polar contact with the O6 of L-Gal (8). This Thr residue is replaced with a histidine in the *Bb*GH95 α-L-fucosidase (4, 5) and in the sequences of the α-L-fucosidases investigated in this study. Residue numbering is based on *Bb*GH95 full-length protein.

Supplemental References

1. **Attia MA, Brumer H.** 2016. Recent structural insights into the enzymology of the ubiquitous plant cell wall glycan xyloglucan. Current Opinion in Structural Biology **40:**43-53.
2. **Campanella JJ, Bitincka L, Smalley J.** 2003. MatGAT: An application that generates similarity/identity matrices using protein or DNA sequences. Bmc Bioinformatics **4:**4.
3. **Sela DA, Garrido D, Lerno L, Wu S, Tan K, Eom HJ, Joachimiak A, Lebrilla CB, Mills DA.** 2012. Bifidobacterium longum subsp. infantis ATCC 15697 alpha-fucosidases are active on fucosylated human milk oligosaccharides. Appl Environ Microbiol **78:**795-803.
4. **Katayama T, Sakuma A, Kimura T, Makimura Y, Hiratake J, Sakata K, Yamanoi T, Kumagai H, Yamamoto K.** 2004. Molecular cloning and characterization of Bifidobacterium bifidum 1,2-alpha-L-fucosidase (AfcA), a novel inverting glycosidase (Glycoside hydrolase family 95). Journal of Bacteriology **186:**4885-4893.
5. **Nagae M, Tsuchiya A, Katayama T, Yamamoto K, Wakatsuki S, Kato R.** 2007. Structural basis of the catalytic reaction mechanism of novel 1,2-alpha-L-fucosidase from Bifidobacterium bifidum. J Biol Chem **282:**18497-18509.
6. **Larsbrink J, Thompson AJ, Lundqvist M, Gardner JG, Davies GJ, Brumer H.** 2014. A complex gene locus enables xyloglucan utilization in the model saprophyte Cellvibrio japonicus. Mol Microbiol **94:**418-433.
7. **Fan S, Zhang H, Chen X, Lu L, Xu L, Xiao M.** 2016. Cloning, characterization, and production of three -l-fucosidases from Clostridium perfringens ATCC 13124. Journal of Basic Microbiology **56:**347-357.
8. **Rogowski A, Briggs JA, Mortimer JC, Tryfona T, Terrapon N, Lowe EC, Basle A, Morland C, Day AM, Zheng H, Rogers TE, Thompson P, Hawkins AR, Yadav MP, Henrissat B, Martens EC, Dupree P, Gilbert HJ, Bolam DN.** 2015. Glycan complexity dictates microbial resource allocation in the large intestine. Nat Commun **6:**7481.